Asynchronous Control of ERP-Based BCI Spellers Using Steady-State Visual Evoked Potentials Elicited by Peripheral Stimuli

Eduardo Santamaría-Vázquez, Víctor Martínez-Cagigal, Javier Gomez-Pilar, and Roberto Hornero, *Senior Member, IEEE*

***Abstract*— Brain-computer interface (BCI) spellers based on event related potentials (ERPs) are intrinsically synchronous systems. Therefore, selections are constantly made, even when users are not paying attention to the stimuli. This poses a major limitation in real-life applications, in which an asynchronous control is required. The aim of this study is to design, develop and test a novel method to discriminate whether the user is controlling the system (i.e., control state) or is engaged in other task (i.e., non-control state). To achieve such an asynchronous control, our method detects the steady-state visual evoked potentials (SSVEPs) elicited by peripheral stimuli of ERP-based spellers. A characterization experiment was conducted with 5 subjects to investigate general aspects of this phenomenon. Then, the proposed method was validated with 15 subjects in offline and online sessions. Results show that the proposed method provides a reliable asynchronous control, achieving an average accuracy of 95.5% for control state detection during the online sessions. Furthermore, our approach is independent of the ERP classification stage, and to the best of our knowledge, is the first procedure that does not need to extend the duration of the calibration sessions to acquire non-control observations.**

***Index Terms*— Brain–computer interfaces, event-related potentials, asynchrony, control-state detection, steady-state visual evoked potentials, P300.**

Manuscript received April 11, 2019; revised July 30, 2019; accepted August 5, 2019. Date of publication August 12, 2019; date of current version September 6, 2019. This work was supported in part by the Ministerio de Ciencia, Innovación y Universidades and European Regional Development Fund (FEDER) under Project DPI2017-84280-R and in part by the project Análisis y correlación entre el genoma completo y la actividad cerebral para la ayuda en el diagnóstico de la enfermedad de Alzheimer (Interregional cooperation program VA Spain-Portugal POCTEP 2014-2020) of the European Commission and FEDER. The work of E. Santamaría-Vázquez was supported in part by the Personal Investigador en Formación (PIF) Grant from the Consejería de Educación de la Junta de Castilla y León and in part by the European Social Fund. The work of V. Martínez-Cagigal was supported by the Personal Investigador en Formación-Universidad de Valladolid (PIF-UVa) Grant from the University of Valladolid. *(Corresponding author: Eduardo Santamaría-Vázquez.)*

The authors are with the Biomedical Engineering Group, E. T. S. I. Telecomunicación, University of Valladolid, 47011 Valladolid, Spain (e-mail: eduardo.santamaria@gib.tel.uva.es; victor.martinez@gib.tel.uva.es; javier.gomez@gib.tel.uva.es; robhor@tel.uva.es).

This article has supplementary downloadable material available at http://ieeexplore.ieee.org, provided by the author.

Digital Object Identifier 10.1109/TNSRE.2019.2934645

I. Introduction

BRAIN–computer interfaces (BCIs) provide a direct pathway between the brain and an external device. These systems use the neural activity to identify the user's intentions and translate them into commands [1], [2]. Nowadays, the main application of BCI systems is to create a new channel of communication in real time for severely disabled people. BCI systems enhance or restore their capability to relate to their environment [1]. Electroencephalography (EEG) is the most common technique to register the neural activity in BCI systems [1]. EEG uses electrodes to register the electrical signal generated by superficial neurons close to them. This signal is the superposition of rhythmic and transient components that reflect the underlying activity of the brain. Particularly, event-related potentials (ERPs) are the natural response of the brain to different types of events [3]. ERPs elicited by a single visual stimulus (e.g., a brief flash) are known as visual ERPs [3].

The first ERP-based BCI was proposed by Farwell and Donchin [4]. The system used the row-column paradigm (RCP) to determine the intentions of the user. The RCP displays a matrix (i.e., speller) with several commands. The rows and columns of the matrix are randomly highlighted a predefined number of times (i.e., sequences). The user has to stare at the desired command and count the flashes (i.e., target stimuli), while ignoring the other stimuli (i.e., non-target stimuli). Target stimuli elicits visual ERPs in the EEG just after each flash. The signal processing stage detects the visual ERPs and determines the command. This BCI is also named as P300-based speller because of the P300 potential, which is the most prominent peak of visual ERPs elicited by target stimuli [1], [3]. Recent research has improved the accuracy and the speed of this BCI through new stimulation paradigms, signal processing methods or hybrid approaches [5]–[9]. Nevertheless, ERP-based spellers are synchronous systems. They always make a selection for every trial, even when the user is not paying attention to the stimuli. This poses a major limitation for most applications, such as wheelchair control or web browsers, where an asynchronous approach should be a key feature [10], [11]. For this reason, detecting whether the user wants to make a selection with the speller (i.e., control state) or is engaged in other task

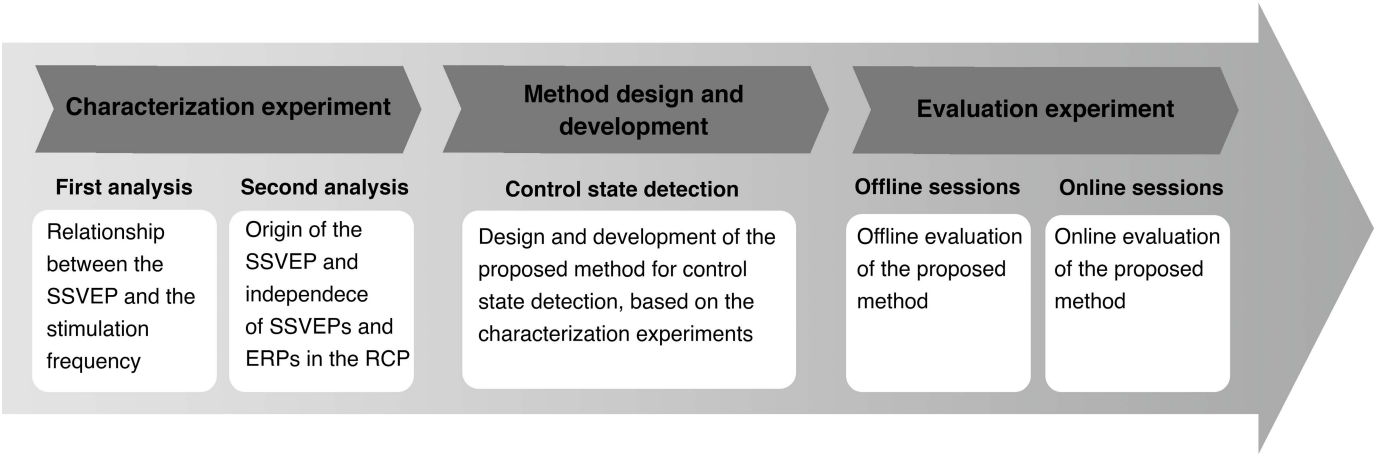

Fig. 1. Overview of the process followed in the study. Firstly, we performed the characterization experiments, in order to describe the characteristics of SSVEPs elicited by the RCP. Secondly, we designed and developed the proposed method for control state detection. Finally, we conducted the evaluation experiment to test the proposed method in offline and online sessions.

(i.e., non-control state) is a crucial issue to bridge the gap between laboratory and real-life BCI applications.

In recent years, several studies have addressed the asynchronous control in ERP-based spellers following two main strategies: (i) algorithms that define a threshold dependent on the output scores of the ERP classification stage [6], [10]–[14]; or (ii) hybrid BCIs that combine different control signals [7], [15], [16]. Nevertheless, these approaches present a number of drawbacks. For instance, algorithms that rely on the output scores of the ERP classification stage have high inter-session variability [5]. Small changes in the amplitude or latency of the ERPs could override the threshold and cause a drastic decrease in the peak accuracy of these methods. In fact, thresholds must be recalibrated before each session with the BCI system. This procedure is time consuming, affects the usability of the system and is frustrating for users [5], [12], [14]. Moreover, previous approaches require to record additional data of the non-control state of the users (i.e., non-control trials) to calculate the threshold, increasing the duration of calibration sessions. On the other hand, hybrid BCIs increase the complexity of the system, requiring different stimulation interfaces. In these BCIs, the user has to be able to manage with two or more control signals, making them more demanding. Consequently, hybrid BCIs might be a major challenge for certain users who cannot maintain high levels of concentration [6], [17]. Algorithms independent of the ERP classification stage may help to overcome these limitations. In this regard, Pinegger *et al.* [18] proposed a method based on the hypothesis that the flashing frequency of the RCP should be represented somehow in the EEG, reaching an average accuracy of 79.5% for control state detection. However, this method still needs to double the duration of the calibration sessions in order to acquire non-control trials.

The aim of this study is to design, develop and test a novel method for control state detection to overcome the limitations of previous approaches. We hypothesize that peripheral stimuli (i.e., non-target stimuli) of ERP-based spellers elicit a weak steady-state visual evoked potential (SSVEP). SSVEPs are waveforms, similar to a sinusoid, that appear with repetitive visual stimuli in the EEG [3], [19], [20]. In order to test the hypothesis, we performed a characterization experiment to study the cause of this phenomenon and its dependence on the stimulation frequency. Finally, we designed and developed a novel method for asynchronous control based on the detection of the SSVEPs elicited by peripheral stimuli. Our approach is independent of the ERP classification stage and does not use additional control signals. Furthermore, to the best of our knowledge, it is the first asynchrony algorithm that does not need to extend the duration of the calibration sessions to acquire non-control trials. The efficacy of the method was tested in offline and online experiments.

II. Methods

This section details the experiments and the proposed method for control state detection. Fig. 1 gives an schematic overview of the work flow followed in this study.

A. Signal Acquisition and Subjects

This study consists of 2 tests: characterization and evaluation experiments. For the characterization experiment, EEG signal was recorded using 16 active electrodes: F3, Fz, F4, C3, Cz, C4, CPz, P3, Pz, P4, PO3, PO7, POz, PO4, PO8 and Oz, according to the extended International 10-20 System distribution. Two electrodes in FPz and the earlobe were used as ground and reference, respectively. This distribution was chosen to favor the detection of the SSVEPs [19]. For the evaluation experiment, EEG signals were recorded using 8 active electrodes, placed at Fz, Cz, Pz, P3, P4, PO7, PO8 and Oz. This configuration was not only chosen based on the results of the characterization experiment, but also because it is commonly used in ERP-based spellers [11], [12]. A g.USBamp (g.Tec, *Guger Technologies*, Austria) was used to amplify and convert the signal into the digital domain with a sampling frequency of 256 Hz. A novel BCI platform, MEDUSA®, was developed and used to present the stimuli, record and save the data and process the signal during the online sessions [21].

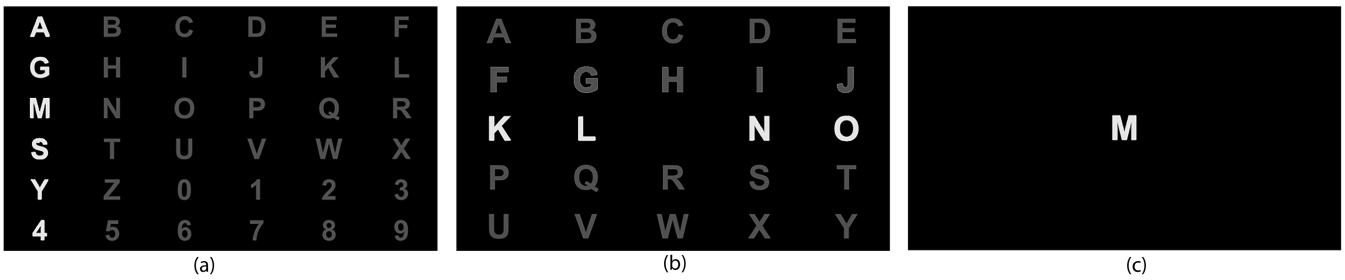

Fig. 2. Matrices used during the experiments: (a) RCP matrix, (b) overt matrix, (c) covert matrix.

TABLE I
STIMULATION PARAMETERS FOR THE CHARACTERIZATION EXPERIMENT

Run	SOA	Inter-stimulus time	Stimulus duration	Flashing frequency
1	475 ms	400 ms	75 ms	2.10 Hz
2	375 ms	300 ms	75 ms	2.67 Hz
3	275 ms	200 ms	75 ms	3.64 Hz
4	175 ms	100 ms	75 ms	5.71 Hz
5	150 ms	75 ms	75 ms	6.66 Hz
6	125 ms	50 ms	75 ms	8.00 Hz

SOA: stimulus onset asynchrony

Twenty healthy subjects participated in the experiments, divided into two groups. Five subjects (mean age: 31.2 ± 4.8 years; 4 males; 1 female) took part in the characterization experiment. The remaining 15 subjects (mean age: 26.1 ± 2.3 years; 11 males; 4 females) took part in the evaluation sessions. The experimental protocol was approved by the local ethics committee and all participants gave their informed consent.

B. Characterization Experiment

The characterization experiment was aimed at analizing the SSVEPs elicited by the RCP. The stimulation frequency of ERP-based spellers is reflected in the EEG and can be used to determine the control state in an asynchronous BCI system [18]. However, the origin and characteristics of this phenomenon have not been studied yet. We hypothesize that non-target stimuli of RCP trigger a weak SSVEP in the user's EEG. Based on this assumption, two analyses were conducted:

1) First Analysis: This analysis was designed to investigate how the characteristics of the SSVEP vary as a function of the stimulation frequency. This frequency is the inverse of the stimulus onset asynchrony (SOA), which is the time between two consecutive flashes calculated as the sum of the stimulus duration and inter-stimulus time. Therefore, the stimulation frequency is defined as $f_{st} = 1/\text{SOA}$. Participants had to spell 6 words (i.e., runs) of 6 letters (i.e., trials) using the matrix shown in Fig. 2a. In one trial, each row and column was highlighted 15 times (i.e., sequences). Each run had a different stimulation frequency, ranging from 2.10 to 8 Hz, as shown in Table I.

2) Second Analysis: This analysis was designed to find out the cause that provokes the SSVEPs and assess their independence from transient ERPs. Four runs were performed with different stimulation matrices in order to analyze separately the two different brain responses elicited by the RCP: transient ERPs, including P300 potentials, and SSVEPs. As previously, each run had 6 trials of 15 sequences. SOA was fixed to 175 ms ($f_{st} = 5.71$Hz) [18]. For the first run, the overt matrix shown in Fig. 2b was used. Participants were asked to stare at the black space while the rows and columns were highlighted. Therefore, participants only saw stimuli with their peripheral visual field. For the second run, the covert matrix shown in Fig. 2c was used. This matrix only had one letter in the centre. Participants were asked to fix the gaze in this letter while it was randomly highlighted. Unlike in the first run, participants only saw stimuli in the central region of their visual field. The last two runs consisted of one control run and one non-control run, using the RCP matrix shown in Fig. 2a. In the control run, participants were asked to spell 6 characters, while in the non-control run, participants were watching a video. In these runs, the left half of the screen showed the video, while the right half displayed the stimulation matrix (see the video added as supplementary material). This analysis was intended to study whether the SSVEPs are provoked by the peripheral stimuli of the RCP and assess their independence from transient ERPs. In that case, the EEG signal in the overt mode should only show the SSVEP, but no ERPs with the P300 component would be found. Conversely, the EEG signal of the covert mode should only contain ERPs, but no SSVEP. Accordingly, the control mode would show the superposition of the SSVEP and ERPs, while in the non-control mode none of these waveforms should be found.

C. Proposed Method for Control State Detection

The Oddball Steady Response Detection (OSRD) method is our novel algorithm for detecting the user's control state in ERP-based spellers. OSRD provides a binary output $y \in \{0, 1\}$ for each trial. When control state is detected ($y = 1$), the system selects a command. Conversely, when non-control state is detected ($y = 0$), no further actions are taken. OSRD takes the EEG signal corresponding to one trial as input (i.e., signal from the first stimulus of the first sequence to the last stimulus of the last sequence considered), and performs in real time the following stages:

1) Pre-Processing: The objective of this stage is to increase the signal-to-noise ratio. Finite impulse response (FIR) band-pass filter is applied between $[f_{st} - bw_1/2,\ f_{st} + bw_1/2]$ Hz, where bw_1 is heuristically set to 2 Hz and $f_{st} = 1/\text{SOA}$.

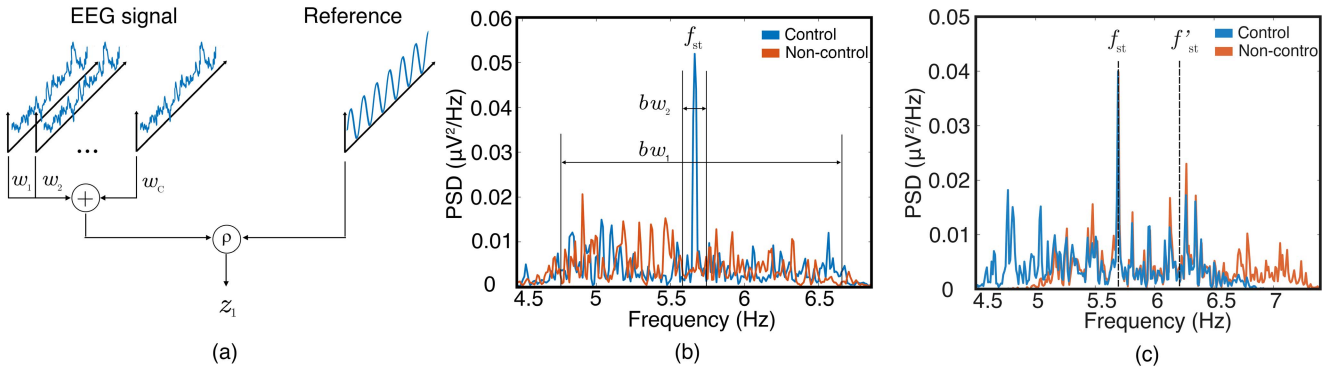

Fig. 3. (a) Schematic representation of the canonical correlation analysis (CCA) used to extract the first feature z_1, where EEG signal represent one trial of dimensions ($C \times N$) and the reference signal is an ideal sinusoid $y = \sin(2\pi \cdot f_{st} \cdot t)$ of dimensions ($1 \times N$). (b) Power spectral density (PSD) of one control and one non-control trials. Parameters bw_1 and bw_2 are used to calculate the second feature z_2. (c) Shifting of the stimulation frequency f_{st} to calculate a synthetic non-control observation from one control trial.

Common Average Reference (CAR) is applied to remove common noisy components in the EEG [12].

2) Feature Extraction: The proposed method extracts two features for each trial, which are based on canonical correlation analysis (CCA) and power spectral density (PSD). CCA is a multivariate statistical method that finds underlying correlations between two multidimensional sets [22]. CCA has been successfully applied in SSVEP-based BCIs [23], [24]. However, to the best of our knowledge, it has not been applied to asynchronous ERP-based spellers yet. In this study, $\boldsymbol{X} \in \mathbb{R}^{C \times N}$ denotes the EEG signal corresponding to one trial, where C is the number of channels and N is the length of the trial. On the other hand, $\boldsymbol{y} \in \mathbb{R}^{1 \times N}$ is the reference signal, which is a sine wave of frequency f_{st}. $\boldsymbol{X}$ and $\boldsymbol{y}$ are normalized (i.e., z-score) to have mean equal to 0 and variance equal to 1. Let $\boldsymbol{x} = \boldsymbol{w}^T \boldsymbol{X}$ denote linear combinations of $\boldsymbol{X}$, where $\boldsymbol{w} \in \mathbb{R}^{C \times 1}$. CCA determines the optimal weight vector $\boldsymbol{w}$ that maximize the Pearson correlation coefficient ρ between $\boldsymbol{x}$ and $\boldsymbol{y}$. A schematic representation is depicted in Fig. 3a describing how CCA is applied in this study. The first feature (z_1) is the maximum correlation coefficient between the trial and the reference, which is calculated by solving the following eigenvalue problem [22]:

$$z_1 = \max_{\boldsymbol{w}} \rho(\boldsymbol{x}, \boldsymbol{y}) = \max_{\boldsymbol{w}} \frac{\boldsymbol{w}^T \boldsymbol{X} \boldsymbol{y}^T}{\sqrt{\boldsymbol{w}^T \boldsymbol{X} \boldsymbol{X}^T \boldsymbol{w}} \sqrt{\boldsymbol{y} \boldsymbol{y}^T}} \tag{1}$$

The second feature (z_2) is directly derived from the spectrum estimation. Firstly, all channels of the trial are concatenated in a single vector of dimensions $(N \cdot C) \times 1$. Secondly, the PSD of this vector is estimated using the Welch's method. The concatenation of the channels allows increasing the spectral resolution. Afterward, z_2 is calculated as the difference between the mean value of the PSD in a narrow range and the mean value in a wide range (see Fig. 3b), formally:

$$z_2 = \frac{1}{bw_2} \int_{f_{st}-bw_2/2}^{f_{st}+bw_2/2} S(f)df - \frac{1}{bw_1} \int_{f_{st}-bw_1/2}^{f_{st}+bw_1/2} S(f)df, \tag{2}$$

where $S(f)$ is the PSD, and bw_1 and bw_2 are fixed to 2 Hz and 0.1 Hz, respectively. In practice, these values are chosen to have enough points of the PSD within these bands, making the method more robust against noise.

3) Synthetic Non-Control Observations: ERP-based spellers should be recalibrated frequently owing to the high variability of ERPs [5]. In fact, users have to spell several trials before each BCI session to assure maximum performance. This procedure is time consuming and frustrating for users [5]. Moreover, previous asynchronous ERP-based spellers needed to extend the duration of calibration sessions to acquire non-control trials. Here, we introduce a new approach in order to create synthetic non-control observations from control trials. Consequently, there is no need to register non-control trials in calibration sessions, which is a great advantage in real-life applications. The aforementioned features (i.e., z_1 and z_2) are calculated based on the stimulation frequency, f_{st}. Assuming that the PSD from the EEG maintains its characteristics in a narrow band around f_{st}, non-control observations can be simulated by shifting the stimulation frequency a fixed value f_0 (see Fig. 3c): $f'_{st} = f_{st} + f_0$, where f_0 is heuristically set to 0.5 Hz. Therefore, f'_{st} is separated enough from f_{st} to consider the spurious power of the SSVEP negligible, while maintaining similar spectral features. Afterward, this value is used in Eq. 1 and Eq. 2 to calculate z_1 and z_2. This procedure is based on the assumption that the characteristics of the PSD at f'_{st} would be similar to non-control trials. Hence, this approach uses control trials to create synthetic non-control observations.

4) Feature Classification: The last stage determines the control state for each observation ($y \in \{0, 1\}$). Linear discriminant analysis (LDA) is a linear classifier that applies dimensionality reduction by projecting the data to simultaneously minimize the within-class covariance and maximize the between-class covariance [25]. In this study, LDA is applied due to its extensive use in BCI systems [11], [12], [14], [18]. Previously, input features are normalized using z-score.

D. Command Selection Algorithm

In this study, we used stepwise linear discriminant analysis (SWLDA) for command selection, which is a reliable and widely accepted methodology [12], [14], [18]. In the

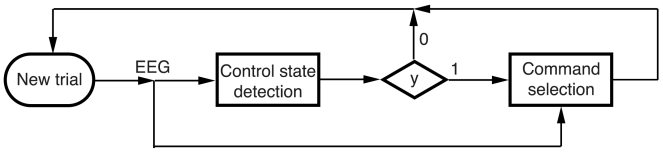

Fig. 4. Flowchart of the overall signal processing algorithm. The control state detection method, OSRD, is independent from the command selection stage, which allows an easy integration in synchronous ERP-based spellers.

preprocessing stage, frequency (i.e., band-pass, 0.5-30 Hz, FIR) and spatial filtering (i.e., CAR) are applied. In the feature extraction stage, a subsampling to 20 Hz over signal epochs of 800 ms from the stimulus onset is applied. The features of each channel are concatenated to make an observation. In the feature selection stage, backward and forward step-wise regression are applied to select the 60 most relevant features for each user. Then, these features are fed to an LDA to detect the ERPs within each epoch, which is labelled with the code of the highlighted row or column. Finally, the algorithm selects the command corresponding to the row and column that reaches the highest score in the classification stage. Further information about this methodology can be found in [12], [14]. It should be noted that the system only selects a command whether control state is determined previously. Fig. 4 shows the flowchart of the overall signal processing algorithm, including control state and command detection stages.

E. Evaluation Experiment

1) Offline Sessions: Offline sessions were aimed at: (i) analizing the performance of OSRD method, (ii) validating the synthetic non-control observations approach, and (iii) acquiring data to train OSRD method for the online session. Fifteen participants performed 10 control and 10 non-control runs in 2 sessions. Each run had 6 trials of 15 sequences. In control runs, participants were asked to spell 6 random characters using the matrix shown in Fig. 2a. In non-control runs, participants had to ignore the stimuli while watching a video or reading a text. In these sessions, the left half of the screen showed the video or the text, while the right half displayed the stimulation matrix (see the video added as supplementary material). In total, 60 control and 60 non-control trials were registered per participant. Two analyses were performed to assess the performance of OSRD method and validate the synthetic non-control observations approach. In the first analysis, leave-one-out (LOO) procedure was applied in the whole dataset for each user, using control and non-control trials (i.e., 120 trials). In each iteration, the classifier was trained using complete trials (i.e., 15 sequences). However, testing features were calculated for each number of sequences. In the second analysis, the evaluation procedure was modified as follows: The training features were calculated only with the control trials, creating from them synthetic non-control observations. When LOO procedure leaved one synthetic non-control observation out for testing, it was replaced by one real non-control observation. Therefore, OSRD was trained with synthetic non-control observations but tested with real non-control observations.

2) Online Sessions: Online sessions were aimed at assessing the efficacy of OSRD in a real setting. To this end, the same participants of the offline experiments performed 4 random words of 6 letters (i.e., 24 trials) using the matrix shown in Fig. 2a. During the first 3 trials of each word, participants had to attend the stimuli. Conversely, during the last 3 trials, participants had to ignore the stimuli while reading a text. As previously, the video or text and the stimulation matrix were displayed in the same screen (see the video added as supplementary material). Control state detection (i.e., OSRD) and command selection (i.e. SWLDA) stages were calibrated using the control trials of the offline dataset (i.e., 60 trials). Hence, the training set of OSRD method included 60 real control observations and 60 synthetic non-control observations. The optimal number of sequences for each participant was determined as the minimum to reach a training accuracy of 95% in command selection. For those who did not reach this threshold, the number of sequences was set to 15.

III. Results

Results of the characterization experiment are shown in Fig. 5 and Fig. 6. The former depicts the SSVEPs for each stimulation frequency of the first characterization analysis. Graphs on the left show the average PSD of all trials, channels and participants. Topographic plots on the right show the normalized power of SSVEPs per channel (i.e., peak value of the PSD at the stimulation frequency) averaged for all trials and participants. Fig. 6 presents the differences in the EEG signal among the 4 different settings of the second analysis (i.e., overt, covert, control, non-control) across all participants in channel Cz. In the upper part, the averaged epochs corresponding to target (i.e. blue lines) and non-target (i.e. red lines) stimuli are shown. The bottom part of the figure displays the average PSD.

Results of the offline experiments for control state detection are presented in Table II. Test accuracies achieved by OSRD in the two performed analyses are shown for 1, 5, 10 and 15 sequences. The stimulation frequency was set to 5.71 Hz.

Results of the online experiments are summarized in Table III. The results of the control state detection stage and the overall system are broken down. The results for control state detection include the accuracy (ACC_1), positive predictive value (PPV), negative predictive value (NPV), true positive rate (TPR) and true negative rate (TNR) achieved by OSRD method during the online sessions. In this analysis, control state has been considered as the positive class and the non-control state as the negative class. Results of the overall system include the control state detection and command selection stages. Hence, control trials were considered correct whether the control state and the command were correctly determined at the same time. For the overall system, accuracy (ACC_2) and information transfer rate (ITR) are given. ITR, expressed in bits/min, measures the amount of information conveyed by a BCI system per unit of time [1]:

$$ITR = (\log_2 N_s + P \log_2 P + (1-P) \log_2 \frac{1-P}{N_s - 1}) S, \quad (3)$$

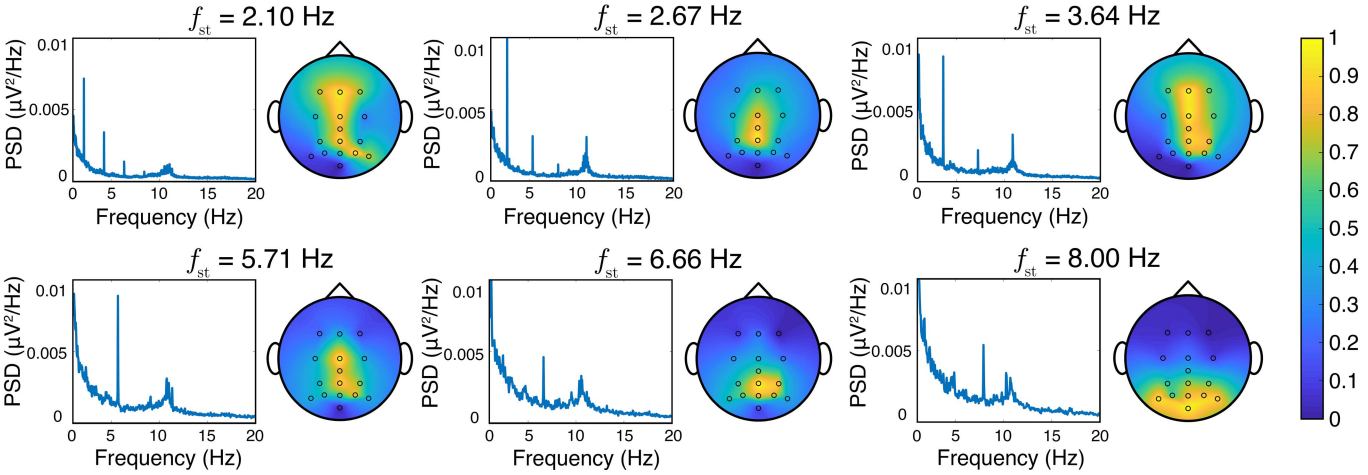

Fig. 5. SSVEPs for different stimulation frequencies. Graphs on the left show the grand average of the PSD for all trials, channels and participants. Topographic plots on the right show the normalized peak value of the PSD at the stimulation frequency averaged for all trials and participants.

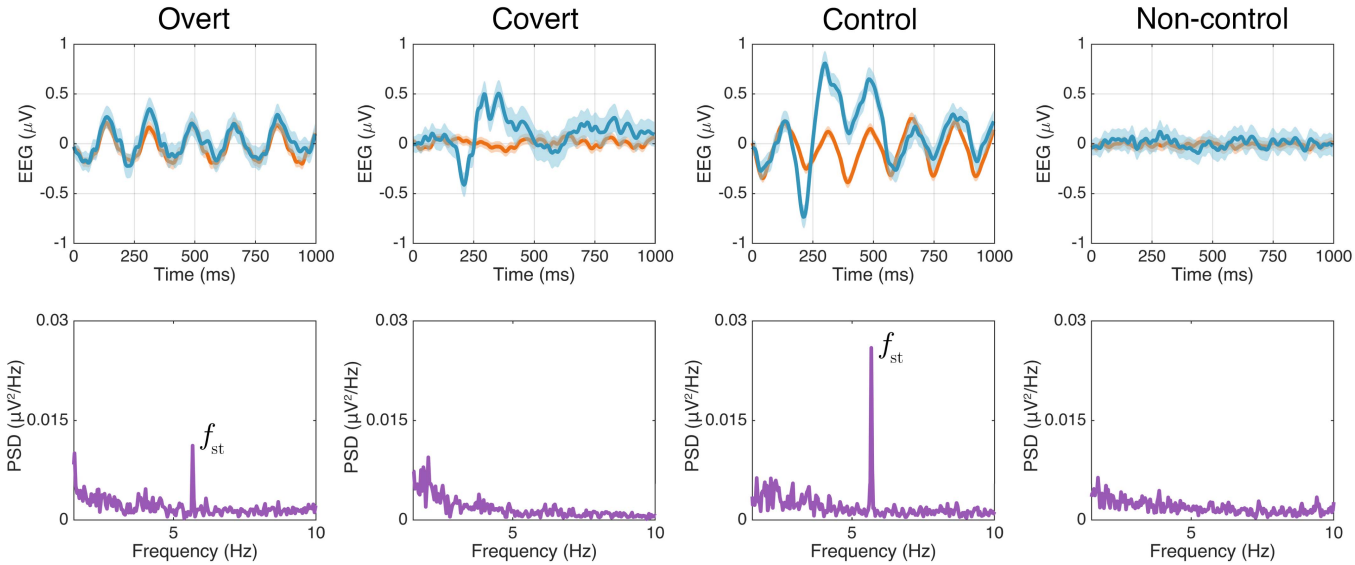

Fig. 6. Temporal and spectral representation of the ERPs in overt, covert, control and non-control modes averaged across all participants of the characterization experiment. In the upper part of the figure, blue lines show the averaged epochs (i.e., 1000 ms after stimuli) corresponding to target stimuli in channel Cz, whereas red lines correspond to non-target stimuli. The shaded area represents the 95% confidence interval. The bottom part of the figure shows the averaged PSD in channel Cz. The stimulation frequency in overt and control modes was 5.71 Hz.

where N_s is the number of targets, P is the classifier accuracy, and S is the number of selections per minute. ITR is valid in memoryless systems, where all possible selections are equally probable [26]. Our system meets both assumptions and thus, ITR is applicable. As in offline sessions, the stimulation frequency was set to 5.71 Hz.

IV. Discussion

In this study, we investigated SSVEPs elicited by the RCP in order to determine the control state in ERP-based spellers. Firstly, we performed two analyses in order to characterize this phenomenon. Afterward, we proposed and evaluated a novel method for control state detection that detects this waveform to achieve an asynchronous control of ERP-based spellers. In the following subsections, we discuss the main results of this study, providing a comprehensive comparison with the state-of-the-art. Finally, the main limitations and future work are also explained.

A. Characterization Experiment

Two different analyses were performed in order to study SSVEPs elicited by the RCP. The first analysis assessed how the variation of the stimulation frequency affected the SSVEPs. As can be seen in Fig. 5, the SSVEP is observable for all analyzed frequencies. The power of the SSVEP is noticeably higher for lower stimulation rates, being maximum at 2.67 Hz, while it is reduced for 6.66 Hz and 8.00 Hz. This tendency seems to be in accordance with the work of Zhang *et al.* [20], who demonstrated that peripheral flickering stimuli at 15 Hz trigger SSVEPs of significantly lower power than those in the central region of the visual field. In addition, harmonics are noticeable in the grand average

TABLE II
OFFLINE TEST ACCURACIES

	No. Sequences							
	1		5		10		15	
	R	S	R	S	R	S	R	S
U01	55.0	54.2	84.2	85.0	98.3	98.3	99.2	99.2
U02	60.8	59.2	88.3	89.2	95.8	95.8	97.5	97.5
U03	63.3	64.2	94.2	95.0	97.5	97.5	100	100
U04	64.2	64.2	83.3	84.2	96.7	95.8	99.2	99.2
U05	61.7	60.8	87.5	87.5	96.7	96.7	97.5	98.3
U06	65.8	64.2	95.8	95.0	96.7	96.7	98.3	98.3
U07	56.7	58.3	75.0	75.8	79.2	76.7	87.5	86.7
U08	63.3	62.5	97.5	97.5	100	100	100	100
U09	61.7	60.0	89.2	88.3	91.7	92.5	95.0	97.5
U10	50.8	50.0	80.8	80.0	88.3	89.2	88.3	88.3
U11	65.0	65.8	91.7	91.7	100	100	100	100
U12	60.0	61.7	79.2	80.0	86.7	85.8	92.5	92.5
U13	65.0	65.0	79.2	78.3	90.0	90.0	95.0	95.0
U14	60.0	56.7	94.2	95.0	99.2	98.3	100	100
U15	73.3	72.5	96.7	96.7	99.2	99.2	100	100
Mean	**61.8**	**61.3**	**87.8**	**87.9**	**94.4**	**94.2**	**96.7**	**96.8**
±SD	5.0	5.2	7.0	6.9	5.8	6.2	4.1	4.2

Accuracies for control state detection (%), R: training and testing with real non-control observations, S: training with synthetic non-control observations but testing with real non-control observations.

TABLE III
ONLINE EXPERIMENT RESULTS

	N_s	Control State Detection					Overall	
		ACC_1	PPV	NPV	TPR	TNR	ACC_2	ITR
U01	10	100	100	100	100	100	91.7	12.4
U02	10	95.8	100	92.3	91.7	100	91.7	12.4
U03	8	100	100	100	100	100	95.8	16.8
U04	10	91.7	100	85.7	83.3	100	91.7	12.4
U05	12	91.7	100	85.7	83.3	100	83.3	8.7
U06	10	95.8	100	92.3	91.7	100	91.7	12.4
U07	15	95.8	92.3	100	100	91.7	95.8	9
U08	8	95.8	92.3	100	100	91.7	95.8	16.8
U09	12	95.8	92.3	100	100	91.7	95.8	11.2
U10	15	91.7	91.7	91.7	91.7	91.7	91.7	8.2
U11	10	95.8	100	92.3	91.7	100	95.8	13.4
U12	10	91.7	91.7	91.7	91.7	91.7	91.7	12.4
U13	8	100	100	100	100	100	100	18.5
U14	12	95.8	100	92.3	91.7	100	91.7	10.3
U15	10	95.8	92.3	100	100	91.7	83.3	10.5
Mean	**10.7**	**95.5**	**96.8**	**94.9**	**94.5**	**96.7**	**92.5**	**12.4**
±SD	2.1	2.8	3.9	5.2	5.8	4.1	4.4	2.9

N_s: number of sequences, Control State Detection: results of control state detection using OSRD method, ACC_1: accuracy (%), PPV: positive predictive value (%), NPV: negative predictive value (%), TPR: true positive rate (%), TNR: true negative rate (%), Overall: results of the overall system including control state detection and command selection, ACC_2: accuracy of the overall system, ITR: information transfer rate (bits/min).

for 2.10 Hz, 2.67 Hz and 3.54 Hz. These results explain our choice of stimulation frequency for the evaluation experiment. Table IV shows a comparative between the average SSVEP power and the time required to select a command using one stimulation sequence for each SOA, according to the first analysis of the characterization experiment. Despite the fact that the maximum average power is reached for $f_{st} = 2.67$ Hz (SOA = 375 ms), which could enhance control state detection, this would reduce the speed for command selection. Comparatively, the average SSVEP power is very similar when $f_{st} = 5.71$ Hz (SOA = 175 ms), while the speed of selection is doubled. Accordingly, $f_{st} = 5.71$ Hz was chosen for the offline and online experiments. Moreover, this value is in accordance with related studies [13], [14], [18]. Regarding the spatial distribution of the SSVEPs, we can point out several

TABLE IV
COMPARATIVE OF THE SSVEP POWER AND SPEED OF SELECTION

SOA	Stimulation frequency	SSVEP power	Selection time
475 ms	2.10 Hz	0.007 $\mu V^2/Hz$	5.55 s
375 ms	2.67 Hz	0.010 $\mu V^2/Hz$	4.55 s
275 ms	3.64 Hz	0.008 $\mu V^2/Hz$	3.33 s
175 ms	5.71 Hz	0.009 $\mu V^2/Hz$	2.00 s
150 ms	6.66 Hz	0.004 $\mu V^2/Hz$	1.78 s
125 ms	8.00 Hz	0.005 $\mu V^2/Hz$	1.49 s

SSVEP power: averaged power of the SSVEP across all participants in the first analysis of the characterization experiment, SOA: stimulus onset asynchrony, Selection time: time required to select a command with one sequence of stimulation.

insightful implications. SSVEPs reach higher amplitudes in the midline electrodes of the frontal, central and parietal areas of the brain (i.e., Fz, Cz, CPz, Pz) for lower frequencies (i.e., 2.10 Hz, 2.67 Hz, 3.64 Hz, 5.71 Hz). However, as the stimulation frequency increases, SSVEPs reach a higher power in the electrodes closer to the visual cortex, located in the occipital lobe (i.e., POz, PO7, PO8, Oz). In summary, results of the first analysis of the characterization experiment show that the RCP used in ERP-based spellers elicits a SSVEP for stimulation frequencies down to 2.71 Hz. In addition, these SSVEPs reach higher power in the frontal central and parietal areas for the lower frequencies. By contrast, scientific literature mostly reports that SSVEPs appear with stimulation frequencies higher than 6 Hz, being mainly located in the visual cortex of the brain, which is in the occipital area [23], [27]–[29]. This discrepancy could be explained by fundamental differences in the stimulation paradigm. The traditional stimulation paradigm used in the majority of studies uses a flickering target where the user has to stare at in order to elicit the SSVEPs, and thus, no cognitive functions are involved [2]. By contrast, in the RCP, the user has to discriminate between target and non-target stimuli to select the command. We hypothesize that, for low frequencies of stimulation, the user has time to consciously discriminate between these two types of stimuli, involving the frontal and central areas of the brain, which are more related to complex cognitive processes and decision making [30]. As the stimulation frequency increases, this conscious discrimination is no longer possible, and the activity is concentrated in the primary visual cortex. In this regard, to the best our knowledge, this is the first study that analyzes the frequency range and spatial distribution of SSVEPs elicited by the RCP. However, numerous studies have reported that different stimulation paradigms can modify the frequency range, amplitude and brain sources of other evoked potentials [31]–[34].

Regarding the second analysis (see Fig. 6), the presence of the SSVEP in the overt mode implies that the cause of this waveform are the non-target stimuli of the visual odd-ball paradigm perceived with the peripheral visual field. As expected, covert mode only elicits transient ERPs, including the P300 potential, which are usually used by the command selection stage to detect which command the user wants to select. Moreover, the linear superposition of these two waveforms explains the shape of the averaged EEG signal in

TABLE V
COMPARATIVE OF PREVIOUS METHODS FOR ASYNCHRONOUS CONTROL OF ERP-BASED SPELLERS

Study	Asynchrony method	Subjects	Independent of ERP classification	Extended calibration sessions	ACC†	FPR†	ACC*	ITR*
Zhang et al. 2008 [10]	Probabilistic analysis	4 CS	No	Yes	–	0.71 epm	–	15.0 bpm
Aloise et al. 2011 [11]	Threshold LDA scores	11 CS	No	Yes	–	0.26 epm	–	11.2 bpm
Martínez-Cagigal et al. 2017 [12]	Threshold LDA scores	5 CS 16 MDS	No	Yes	– –	– –	95.75% 84.14%	– –
Tang et al. 2018 [35]	Threshold LDA scores	4 CS	No	Yes	–	–	90.30%	–
Aydin et al. 2018 [6]	Threshold LDA scores	10 CS	No	Yes	–	–	93.27%	43.1 bpm
Martínez-Cagigal et al. 2019 [14]	Threshold LDA scores	5 CS 16 MDS	No	Yes	– –	– –	92.30% 80.60%	– –
Pinegger et al. 2016 [18]	SAM HAM	21 CS	Yes No	Yes Yes	79.5% 95.5%	– –	– –	– –
Present study	**OSRD**	**15 CS**	**Yes**	**No**	**95.5%**	**0.14 epm**	**92.5%**	**12.4 bpm**

SAM: spectral analysis method, HAM: hybrid analysis method, CS: control subjects, MDS: motor disabled subjects, FPR: false positive rate, epm: events per min, ACC: accuracy (%), ITR: information transfer rate, bpm: bits per min, LDA: linear discriminant analysis, OSRD: oddball steady response detection, †Control state detection stage, *Overall system.

control mode. The main implication of this finding is that SSVEPs and ERPs elicited by the RCP are originated by different mechanisms. Thus, OSRD method could be considered independent of the command selection stage. This feature makes OSRD very versatile, since it can be integrated in synchronous ERP-based spellers with different command selection algorithms to achieve a reliable asynchronous control.

B. Evaluation Experiment

Regarding the offline sessions, no significant differences have been found between OSRD trained with real and synthetic non-control observations regardless the number of sequences (Wilcoxon signed-rank test, p-value > 0.05). Thus, synthetic non-control observations may be considered similar to real non-control observations. Furthermore, the use of synthetic non-control observations reduces the duration of calibration sessions by half because the acquisition of non-control trials is no longer needed. Additionally, it should be noted that 13 out of 15 participants reached an accuracy higher than 90%. These characteristics represent a great advantage in real-life BCI applications.

Table III presents the results of the online sessions. OSRD method reached an average accuracy of 95.5% for control state detection. Since the achieved TNR (96.7%) is slightly higher than the TPR (94.5%), OSRD is more reliable when it comes to detecting the non-control state. This could be expected, since users may lose their concentration during the control task, reducing the power of the SSVEP, being the opposite very unlikely. This feature is useful in applications where avoiding false positives is a critical issue, such as wheelchair control. Additionally, Table III also includes the ITR and the accuracy of the overall system. These results show that participants were able to control the ERP-based speller asynchronously without compromising the overall system performance. In fact, 13 out of 15 participants reached an overall accuracy greater than 90%, achieving an average accuracy of 92.5%. Furthermore, this session demonstrated the ability of OSRD to work in real time.

C. Related Work

In this section, we compare previous approaches for asynchronous control of ERP-based spellers with OSRD. Table V shows an overview of these studies. It should be noted that it is difficult to make a direct comparison of these studies due to differences in stimulation paradigms, signal processing and experimental settings. As a first approach, Zhang et al. proposed a system based on the rapid serial visualization paradigm that assessed the statistical differences between the output of a SVM fed with target and non-target epochs [10]. This study achieved an ITR = 15 bits/min and a FPR = 0.71 events/min with 4 control subjects (CS). Despite the suitable ITR, their FPR suggests that the asynchronous management could be improved. In fact, OSRD achieved a FPR = 0.14 events/min in the online session, showing the reliability of our approach. Aloise et al. improved the accuracy of the asynchronous detection, reaching a FPR = 0.26 events/min [11]. However, our approach still improves this value. Martínez-Cagigal *et al.* [12], [14] used the same asynchronous framework, obtaining with CS overall system accuracies of 95.75% and 92.30% respectively. Among the previous studies, Aydin *et al.* [6] reached the highest performance with an ITR = 43.15 bits/min. However, it should be taken into account that they used a different stimulation setting: the region based paradigm (RBP). This paradigm uses regions of commands far from each other and selections are performed in two levels to maximize speed, which makes it difficult to compare their results with the rest of the studies [6]. All previous studies rely on a threshold based on different parameters calculated with the output of the ERP classification stage to determine the control state (i.e., area under the ROC, probability analysis, etc). Despite their usefulness, these approaches present a number of limitations. ERP-based spellers will always be affected to a certain extent by inter-session variability, due to inherent properties of brain signals and external factors, such as cap position or attenuation [2], [5]. However, this variability significantly affects systems that depend on the output scores of the ERP classification

stage to achieve an asynchronous control. The main reason is that the distribution of the output scores changes across sessions, invalidating the threshold. In fact, in our own experience based on previous studies [12], [14], the performance of this approach for asynchronous control is reduced drastically even for consecutive sessions, increasing the number of false negatives. However, without the threshold, the same models could be used for several days with acceptable accuracy. Independent methods of the ERP classification stage would help to overcome these limitations. As stated before, OSRD is included within this kind of approaches. Pinegger *et al.* [18] explored this strategy. In this study, SSVEPs elicited by the RCP were also used to determine the user's control state. They proposed the spectral analysis method (SAM), based on a threshold on the FFT values of averaged epochs of 1000 ms (256 samples). Despite the novelty of this method, its performance (TPR $=$ 88.3%, TNR $=$ 73.7%, ACC $=$ 79.5%, 15 sequences) suggests that the control state detection could be improved. SAM method is the only one in this comparative that allows a direct comparison with OSRD, since it relies on the same phenomenon to determine the control state. In this regard, OSRD method outperforms SAM in all the given metrics (TPR $=$ 94.5%, TNR $=$ 96.7%, ACC $=$ 95.5%, 10.7 sequences). In order to improve their results, Pinegger et al. combined SAM with the ERP classifier scores in the hybrid analysis method (HAM). This method achieved a similar performance to OSRD (TPR $=$ 99.0%, TNR $=$ 93.2%, ACC $=$ 95.5%, 15 sequences). However, HAM still depends on the ERP classification stage, having the same drawbacks that previous approaches. Unlike OSRD, all asynchrony methods included in this comparative need non-control trials to be calibrated, which doubles the duration of training sessions. Furthermore, given their dependence on the ERP classifier, they should be often recalibrated, taking a great amount of time from users and reducing the applicability of these methods in a real context. OSRD addresses this issue by creating synthetic non-control observations from control trials, increasing the usability of the system. Finally, it is worthy to mention that we did not include hybrid BCIs in the comparative, since the use of different control signals does not allow a direct comparison [6], [17].

D. Limitations and Future Work

Despite the positive results achieved in this study, we can point out several limitations. This study failed to test OSRD method with motor disabled people, who would be the target users. In this regard, BCI systems generally present lower performance with motor disabled subjects. Nevertheless, SSVEPs could be less affected than ERPs in this population [36]. OSRD calculates two features based on CCA and spectral analysis. However, novel algorithms for SSVEP detection and complementary metrics based on statistical analysis could improve the performance and should be explored in the future [24], [37]. In this work, we used a reliable and widely accepted methodology for command selection such as SWLDA. However, recent advances in EEG signal processing, such as ensemble classifiers, deep learning or early stopping algorithms, have improved the accuracy and ITR of synchronous ERP-based spellers. In this regard, the integration of OSRD method to achieve an asynchronous control of these spellers could increase the overall accuracy and ITR reached in this study and represents a promising line of future work. Lastly, we acknowledge limitations in the comparison with related studies due to differences in subjects, signal processing and stimulation paradigm. In this regard, a direct comparison with the same subjects and BCI framework would help to draw stronger conclusions regarding performance, and should be done in the future.

V. Conclusion

This study presents a novel method to determine the user's control state by means of the detection of SSVEPs elicited by the RCP in ERP-based spellers. We demonstrated that these waveforms, whose shape and spatial distribution depend on the stimulation frequency, are provoked by peripheral stimuli of the RCP. The proposed method has been validated in offline and online experiments, achieving an average accuracy of 95.5% for control state detection and outperforming other related state-of-the-art methods. Additionally, our approach presents two main advantages: it is independent of the ERP classification stage, reducing the inter-session variability; and it is the first asynchrony method that does not need to register non-control trials, drastically reducing the duration of calibration sessions. These features make OSRD a suitable method to implement asynchronous ERP-based spellers in a real context.

References

[1] J. R. Wolpaw, N. Birbaumer, D. J. McFarland, G. Pfurtscheller, and T. M. Vaughan, "Brain–computer interfaces for communication and control," *Clin. Neurophysiol.*, vol. 4, no. 113, pp. 767–791, 2002.

[2] L. F. Nicolas-Alonso and J. Gomez-Gil, "Brain computer interfaces, a review," *Sensors*, vol. 12, no. 2, pp. 1211–1279, 2012.

[3] S. J. Luck, *An Introduction to the Event-Related Potential Technique*. Cambridge, MA, USA: MIT Press, 2014.

[4] L. A. Farwell and E. Donchin, "Talking off the top of your head: Toward a mental prosthesis utilizing event-related brain potentials," *Electroencephalograph. Clin. Neurophysiol.*, vol. 70, no. 6, pp. 510–523, Dec. 1988.

[5] F. Schettini, F. Aloise, P. Aricò, S. Salinari, D. Mattia, and F. Cincotti, "Self-calibration algorithm in an asynchronous P300-based brain-computer interface," *J. Neural Eng.*, vol. 11, no. 3, 2014, Art. no. 035004.

[6] E. A. Aydin, O. F. Bay, and I. Guler, "P300-based asynchronous brain computer interface for environmental control system," *IEEE J. Biomed. Health Inform.*, vol. 22, no. 3, pp. 653–663, May 2018.

[7] Y. Yu *et al.*, "Self-paced operation of a wheelchair based on a hybrid brain-computer interface combining motor imagery and P300 potential," *IEEE Trans. Neural Syst. Rehabil. Eng.*, vol. 25, no. 12, pp. 2516–2526, Dec. 2017.

[8] E. Yin, T. Zeyl, R. Saab, T. Chau, D. Hu, and Z. Zhou, "A hybrid brain–computer interface based on the fusion of P300 and SSVEP scores," *IEEE Trans. Neural Syst. Rehabil. Eng.*, vol. 23, no. 4, pp. 693–701, Jul. 2015.

[9] M. Xu, X. Xiao, Y. Wang, H. Qi, T. P. Jung, and D. Ming, "A brain–computer interface based on miniature-event-related potentials induced by very small lateral visual stimuli," *IEEE Trans. Biomed. Eng.*, vol. 65, no. 5, pp. 1166–1175, May 2018.

[10] H. Zhang, C. Guan, and C. Wang, "Asynchronous p300-based brain–computer interfaces: A computational approach with statistical models," *IEEE Trans. Biomed. Eng.*, vol. 55, no. 6, pp. 1754–1763, Jun. 2008.

[11] F. Aloise *et al.*, "P300-based brain–computer interface for environmental control: An asynchronous approach," *J. Neural Eng.*, vol. 8, no. 2, 2011, Art. no. 025025.

[12] V. Martínez-Cagigal, J. Gomez-Pilar, D. Álvarez, and R. Hornero, "An asynchronous p300-based brain-computer interface Web browser for severely disabled people," *IEEE Trans. Neural Syst. Rehabil. Eng.*, vol. 25, no. 8, pp. 1332–1342, Aug. 2017.

[13] S. He *et al.*, "A P300-based threshold-free brain switch and its application in wheelchair control," *IEEE Trans. Neural Syst. Rehabil. Eng.*, vol. 25, no. 6, pp. 715–725, Jun. 2017.

[14] V. Martínez-Cagigal, E. Santamaría-Vázquez, J. Gomez-Pilar, and R. Hornero, "Towards an accessible use of smartphone-based social networks through brain-computer interfaces," *Expert Syst. Appl.*, vol. 120, pp. 155–166, Apr. 2019.

[15] R. C. Panicker, S. Puthusserypady, A. P. Pryana, and Y. Sun, "Asynchronous P300 BCI: SSVEP-based control state detection," in *Proc. Eur. Signal Process. Conf.*, 2010, vol. 58, no. 6, pp. 934–938.

[16] Y. Li, J. Pan, F. Wang, and Z. Yu, "A hybrid BCI system combining P300 and SSVEP and its application to wheelchair control," *IEEE Trans. Biomed. Eng.*, vol. 60, no. 11, pp. 3156–3166, Nov. 2013.

[17] S. Amiri, R. Fazel-Rezai, and V. Asadpour, "A review of hybrid brain-computer interface systems," *Adv. Hum.-Comput. Interact.*, vol. 2013, Dec. 2013, Art. no. 187024.

[18] A. Pinegger, J. Faller, S. Halder, S. C. Wriessnegger, and G. R. Müller-Putz, "Control or non-control state: That is the question! An asynchronous visual P300-based BCI approach," *J. Neural Eng.*, vol. 12, no. 1, 2015, Art. no. 014001.

[19] F. B. Vialatte, M. Maurice, J. Dauwels, and A. Cichocki, "Steady-state visually evoked potentials: Focus on essential paradigms and future perspectives," *Prog. Neurobiol.*, vol. 90, pp. 418–438, Apr. 2010.

[20] N. Zhang *et al.*, "Retinotopic and topographic analyses with gaze restriction for steady-state visual evoked potentials," *Sci. Rep.*, vol. 9, no. 1, 2019, Art. no. 4472.

[21] E. Santamaría-Vázquez, V. Martínez-Cagigal, and R. Hornero, "MEDUSA: Una nueva herramienta para el desarrollo de sistemas brain-computer interface basada en python," *Cognit. Area Netw.*, vol. 5, no. 1, pp. 87–92, 2018.

[22] J. D. Jobson, *Applied Multivariate Data Analysis: Categorical and Multivariate Methods*, vol. 2. New York, NY, USA: Springer, 2012.

[23] Z. Lin, C. Zhang, W. Wu, and X. Gao, "Frequency recognition based on canonical correlation analysis for SSVEP-based BCIs," *IEEE Trans. Biomed. Eng.*, vol. 53, no. 12, pp. 2610–2614, Dec. 2006.

[24] Y. S. Zhang *et al.*, "Two-stage frequency recognition method based on correlated component analysis for SSVEP-based BCI," *IEEE Trans. Neural Syst. Rehabil. Eng.*, vol. 26, no. 7, pp. 1314–1323, Jul. 2018.

[25] K. Fukunaga, *Introduction to Statistical Pattern Recognition*. New York, NY, USA: Academic, 2013.

[26] W. Speier, C. Arnold, and N. Pouratian, "Evaluating true BCI communication rate through mutual information and language models," *PLoS ONE*, vol. 8, no. 10, 2013, Art. no. e78432.

[27] G. Bin, X. Gao, Z. Yan, B. Hong, and S. Gao, "An online multi-channel SSVEP-based brain-computer interface using a canonical correlation analysis method," *J. Neural Eng.*, vol. 6, no. 4, 2009, Art. no. 046002.

[28] C. Jia, X. Gao, B. Hong, and S. Gao, "Frequency and phase mixed coding in SSVEP-based brain–computer interface," *IEEE Trans. Biomed. Eng.*, vol. 58, no. 1, pp. 200–206, Jan. 2011.

[29] O. Friman, I. Volosyak, and A. Graser, "Multiple channel detection of steady-state visual evoked potentials for brain-computer interfaces," *IEEE Trans. Biomed. Eng.*, vol. 54, no. 4, pp. 742–750, Apr. 2007.

[30] S. Standring, *Gray's Anatomy E-Book: The Anatomical Basis of Clinical Practice*. Amsterdam, The Netherlands: Elsevier, 2015.

[31] A. Bachiller *et al.*, "Auditory P3a and P3b neural generators in schizophrenia: An adaptive sLORETA P300 localization approach," *Schizophrenia Res.*, vol. 169, nos. 1–3, pp. 318–325, 2015.

[32] A. Mazaheri and T. W. Picton, "EEG spectral dynamics during discrimination of auditory and visual targets," *Cogn. Brain Res.*, vol. 24, pp. 81–96, Jun. 2005.

[33] J. V. Odom, M. Bach, M. Brigell, G. E. Holder, D. L. McCulloch, A. P. Tormene, and Vaegan, "ISCEV standard for clinical visual evoked potentials (2009 update)," *Documenta Ophthalmol.*, vol. 120, no. 1, pp. 111–119, 2010.

[34] J. Polich, "Updating P300: An integrative theory of P3a and P3b," *Clin. Neurophysiol.*, vol. 118, no. 10, pp. 2128–2148, Oct. 2007.

[35] J. Tang, Y. Liu, J. Jiang, Y. Yu, D. Hu, and Z. Zhou, "Toward brain-actuated mobile platform," *Int. J. Hum.-Comput. Interact.*, vol. 35, no. 10, pp. 846–858, 2018.

[36] A. Combaz *et al.*, "A comparison of two spelling brain-computer interfaces based on visual P3 and SSVEP in locked-in syndrome," *PLoS ONE*, vol. 8, no. 9, 2013, Art. no. e73691.

[37] V. Martínez-Cagigal, E. Santamaría-Vázquez, and R. Hornero, "Asynchronous control of P300-based brain–computer interfaces using sample entropy," *Entropy*, vol. 21, no. 3, p. 230, 2019.